

Surface figure measurement of silicon carbide mirrors at cryogenic temperatures

Peter Blake^a, Ronald G. Mink^a, John Chambers^a, F. David Robinson^{a,b},

David Content^a, Pamela Davila^a

^a Goddard Space Flight Center, Code 551, Greenbelt, MD 20771

^b Orbital Sciences Corporation, 7500 Greenway Center Drive, Suite 700, Greenbelt MD 20770

OCIS codes: 120.6650, 120.6810, 230.4040

ABSTRACT

The surface figure of a developmental silicon carbide mirror, cooled to 87 K and then 20 K within a cryostat, was measured with unusually high precision at the Goddard Space Flight Center (GSFC). The concave spherical mirror, with a radius of 600 mm and a clear aperture of 150 mm, was fabricated of sintered silicon carbide. The mirror was mounted to an interface plate representative of an optical bench, made of the material Cesium[®], a composite of silicon, carbon, and silicon carbide. The change in optical surface figure as the mirror and interface plate cooled from room temperature to 20 K was 3.7 nm rms, with a standard uncertainty of 0.23 nm in the rms statistic. Both the cryo-change figure and the uncertainty are among the lowest such figures yet published. This report describes the facilities, experimental methods, and uncertainty analysis of the measurements.

1 INTRODUCTION

A new facility at the Goddard Space Flight Center is designed to measure with unusual accuracy the surface figure of mirrors at cryogenic temperatures down to 12 K. The facility is currently configured for spherical mirrors with a radius of curvature (ROC) of 600 mm, and apertures of about 150 mm or less.

The goals of the currently-reported experiment were to:

- 1) Obtain the best possible estimate of test mirror surface figure, $S(x,y)$ at 87 K and 20 K.

The surface figure is the two-dimensional map of deviation from the best-fit sphere. The terms figure, surface figure, and surface figure error (SFE) are used synonymously.

- 2) Obtain the best estimate of the cryo-change, $\Delta(x,y)$: the change in surface figure between room temperature and the two cryo-temperatures.
- 3) Determine the uncertainty of these measurements, using the definitions and guidelines of the *ISO Guide to the Expression of Uncertainty in Measurement*^{1,2}.

2 TEST MIRRORS AND MOUNTING

Several mirrors have been tested in the facility, in different support conditions. The measurement at 80 K of a silicon foam-core mirror made by the Schafer Corporation in 2001 – an early example of their SLMS™ technology³ – is described in another paper.⁴ The measured cryo-change from room temperature to 80 K was 4.9 nm rms.

More recently, the laboratory has measured two silicon carbide mirrors manufactured by Galileo Avionica (GA) of Florence, Italy,⁵ for the European Space Agency, in a technology demonstration for the Near Infrared Spectrograph (NIRSpec) on the James Webb Space Telescope (JWST). One mirror (figure 1a) was fabricated from a near-net-shape blank of the material Cescic®, manufactured by ECM, in Ottobrun, Germany. The second (figure 1b) was

made of sintered silicon carbide, from a near-net-shape blank manufactured by Bettini SpA, Italy. Both mirrors had a 150mm clear aperture and spherical surface with a 600mm radius. Both mirrors were clad with coatings designed to be polished to the smoothness required by visible light operations (< 2 nm rms surface roughness).

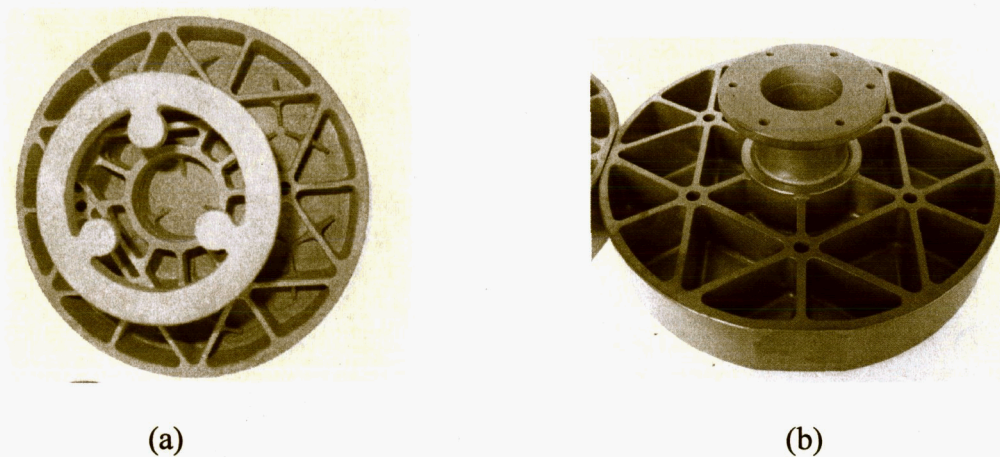


Figure 1: GA test mirrors a) the Cesium mirror, ECM3; b) the SiC mirror, BET2

To support the Cesium interface plate (figure 2a) on which each mirror was fastened, a kinematic mount was designed⁶ that attached to the cold plate (figure 2b). It held the Cesium interface plate with six degrees of freedom such that when the cold plate shrank, no strain was applied to the Cesium plate. A second mount, called the simple support (figure 2c), provided a second support condition: one without the Cesium interface plate. It also attached to the cold plate; and it held the test mirror up on two cylindrical support pegs, while the back of the mirror rested upright against the flat of the support at three unknown points. A safety clip, which did not touch the mirror surface, prevented the mirror from falling out during operations.

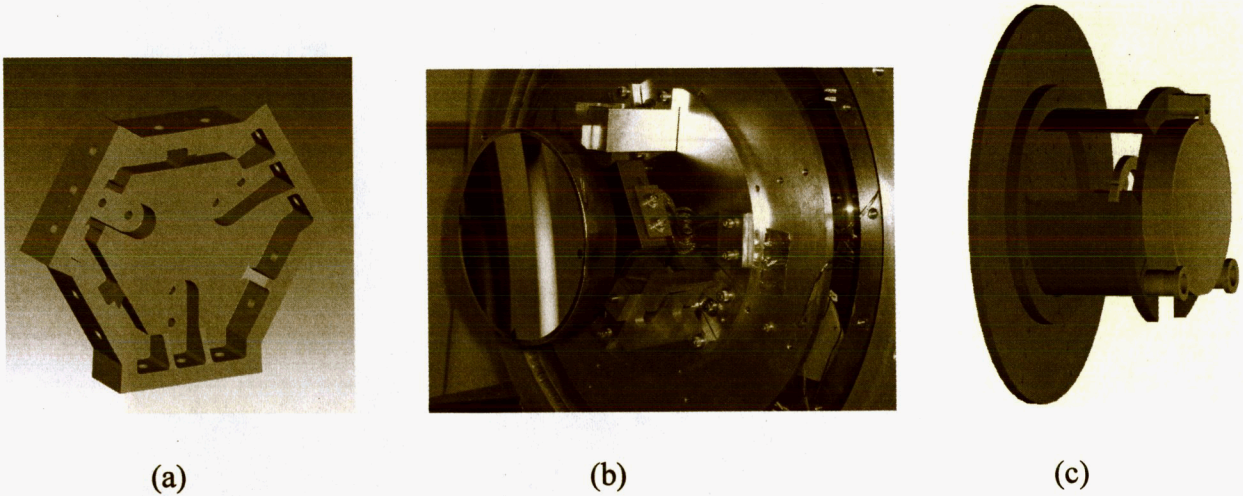


Figure 2: a) the Cesic interface plate; b) BET2, mounted to interface plate, on kinematic mount; c) ECM3, mounted to simple support

3 FACILITY

A Zygo “Verifire AT”[®] phase-measuring interferometer, positioned on crossed rails for x-y-z control (figure 3), focuses through a window into a cryostat (dewar). The cryostat and thermal regulation of the test mirrors is described in another paper⁷. The cryostat has controls to provide tip and tilt about the front face of the window (figure 4) to complete the five axes of alignment. The whole facility rests on a curtained vibration-isolation table.

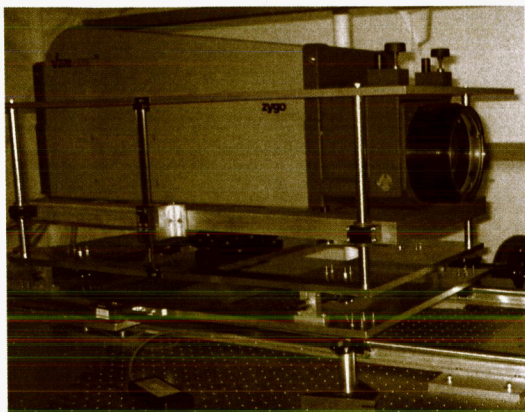


Figure 3: Interferometer on XYZ stage

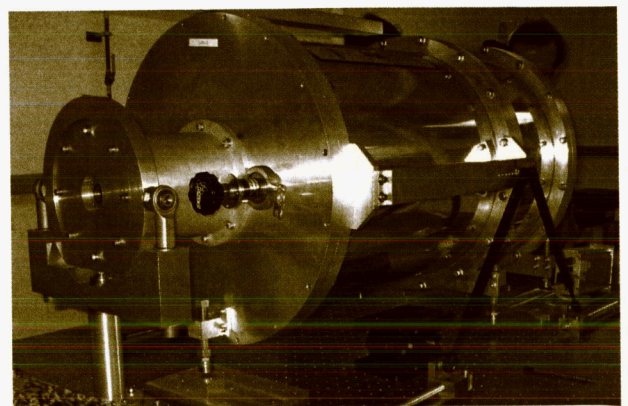


Figure 4: Dewar in tip-tilt sling

We take advantage of the converging interferometer beam for the testing of a 600 mm ROC sphere in using a small thin window placed close to the focal point of the interferometer. There are several significant advantages:

- a a small window can be thinner for a given deflection under vacuum, leading to less spherical aberration;
- b a small footprint of the beam on the window makes it easier to achieve low transmitted wavefront error;
- c placing the window 600mm from the mirror on a narrow extension cylinder lowers the radiative coupling between the cold interior and the window, lessening the mutual distortions of the window and the mirror. The interior surface of the window has a large view of room-temperature metal in the extension, keeping it warm.

The window is fused silica, 0.25 in thickness, AR-coated on both surfaces.

Early ray trace modeling of the test configuration revealed that the aberrations created by the window could be kept under control if the window tilt with respect to the optical axis of the interferometer were kept below 3 arcminutes (see details in section 5). In addition, it was shown that since the window was so small, in order to get the reflected wavefront from the test mirror completely through it, the test mirror must be aligned perpendicular to the window within 40 arcminutes – or the image would be clipped. Both of these requirements were met by careful in-process metrology⁹.

4 TEST MEASUREMENTS

In each support, the two mirrors were subjected to two or three thermal cycles (figure 5), with interferometric measurements of the test mirror surface taken at the following points in each cycle:

RTP: ambient conditions, room temperature, no window, no vacuum (beginning and end of the three-cycle series)

RTV: Test mirror in dewar at room temperature under vacuum. Measurement through the window. (2X, each cycle)

87K: Cold plate with liquid nitrogen plus supplemental heat, mirror at 87 ± 1 K (2X)

20 K: Cold plate with liquid helium plus supplemental heat, mirror at 20 ± 1 K (1X)

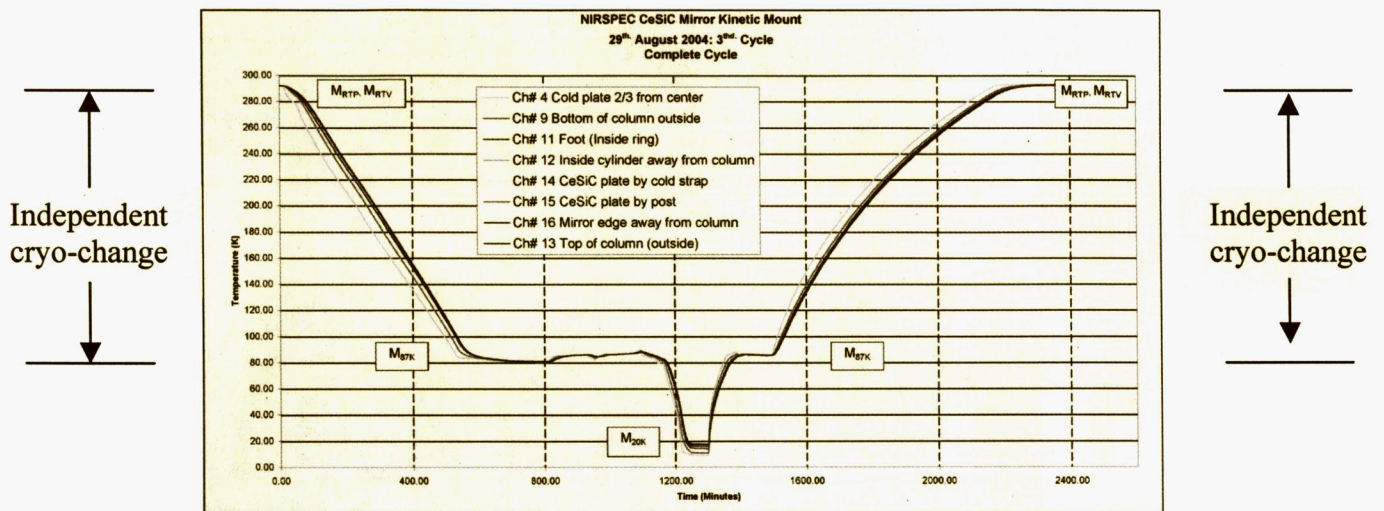


Figure 5: One thermal cycle (repeated 2-3X, each support)

The mirrors were measured at a near-steady-state condition, with the criterion that the rate of change of the mirror fall below 1 K/15 min. For each measurement step of the thermal cycle, twenty successive individual “shots” were taken, each using thirty-two phase averages; and the twenty shots were averaged into a single “measurement”.

5 CORRECTION AND CONTROL OF SYSTEMATIC EFFECTS

The measurements must be corrected for all systematic effects (errors). There are two major corrective factors to be applied to the direct measurements at cryo:

- 1) aberration of the beam as it passes twice through the window of the cryostat, and
- 2) error in the reference surface of the interferometer's transmission sphere.

Estimated error files for window aberration (E_w) and for transmission sphere reference surface (E_T), aligned and scaled with the measurement data set (M_{20K}), are subtracted, as in equation 1:

$$S_{20K} = M_{20K} - E_T - E_w \quad (1)$$

When the cryo-change itself is calculated, as in equation 2, both of these systematic effects are eliminated:

$$\Delta_{20K-RTV} = M_{20K} - M_{RTV} \quad (2)$$

A *Changes in the window*

However, in the calculation of either the cryo-change or the final surface figure, the window aberrations would be imperfectly eliminated if the window changed shape during the cooldown. In order to estimate the changing aberrations as the window distorts under vacuum and cold, both the outside and inside surfaces – as viewed through the thickness – were measured interferometrically during a cryo-run. A substitute window wedged to 0.5° (and no AR-coating) was used to model the mechanical behavior of the real window. At each step of temperature and pressure, a measurement (with 160 phase averages, to limit noise) was made of both window faces.

A Zemax[®] model was prepared for the Fizeau-interferometric test of a 600mm ROC, 150mm diameter spherical mirror. A window identical in its parameters to the test window was placed in the design position; and, using the measured window surface data, the effects of window surface distortion on the modeled wavefront error were determined.

The change in the wavefront error of a test mirror as the window changes between the two temperatures was revealed by the model to be 0.02nm rms – well below measurement

uncertainty limits. Since the wavefront can be aberrated also by a gradient in the index of refraction, n , due to a gradient in the window temperature, it is also important to estimate, bound, or include the possible effect of this change when the cold plate reaches 20K. This small effect is included in the analysis described above, because any wavefront distortions due to dn/dt are captured as surface error in the window's rear surface.

The window's inner surface *did* change measurably between the RT and cryo conditions. Reductions in defocus and spherical aberration and an increase in astigmatism were all found. But the changes create no measurable impact on a test mirror's wavefront error. Full details of the measurement and modeling are in Reference 4.

B Alignment

It was found that if the optic axis were perpendicular to the window of the cryostat, the only aberration that contributes an error in S of greater than 0.4 nm rms is spherical aberration, which contributed an error equal to 8.8 nm rms. However, if the window were tilted, there would be added contributions of coma and astigmatism; and – what is worse – the amount of aberration would depend on the distance of the mirror from the window. Since this distance could change during thermal excursions, without our having any way to measure it, it was determined to keep the angle of the optic axis to the window below 3 *arcmin*, which would allow a maximum error of 0.4 nm rms_[MSOffice1] over and above the aberration at perpendicularity. This bounded error (0.4 nm rms) is incorporated as an element in the uncertainty analysis (section 7).

C Transmission sphere error

In the interferometer itself, the only systematic effect above 0.4 nm rms is imperfection of the reference surface in the transmission sphere. This error can be measured and subtracted

by a technique called “absolute measurement” or the “two-sphere test”^{8,9}. This technique has been performed on our interferometer with two different reference mirrors – two different cavity sizes – and has yielded a map of the interferometer errors, which can be used as a corrective file.

6 DEFINITION OF UNCERTAINTY

The statistics for which we require an estimation of uncertainty are the rms of the cryo-change, Δ , and the rms of the *in situ* surface figure error, S , of the test mirror at cryo-temperature. Analysis of uncertainty is based in the recommendations of NIST and ISO, as in ISO’s “Guide to the Expression of Uncertainty in Measurement” (*GUM*). The basic guidelines relevant to our discussion are the following:

- a Represent each component of uncertainty u_i as an estimated standard deviation.
- b For a systematic effect, the relevant uncertainty is that of the corrective factor.
- c Combine elements using the *law of propagation of uncertainty*, whose most recognizable corollary is that independent elements of uncertainty are added in “root sum square” or “RSS” fashion. The combined uncertainties form the *Combined Standard Uncertainty*, U_c .
- d A confidence interval may be formed from the combined standard uncertainty by multiplying it by a “coverage factor”, typically between two and three, yielding the *Expanded Uncertainty*, U . The confidence intervals for measurements in this report are given as expanded uncertainties, with a coverage factor of three.

7 CRYO-CHANGES AND THEIR UNCERTAINTIES

The discussion of results will focus on the best-performing of the mirrors, the sintered silicon carbide mirror, BET2, with occasional references to other tests. The initial measurement of

BET2 at ambient conditions, corrected for transmission sphere error, yielded a surface figure S of 14.1 nm rms.

A *Cryo-changes*

A “cryo-change” is a map of the changes in surface heights over the pixel space of the mirror surface, as the mirror temperature is lowered from room temperature to a specific cryo-temperature – in our case, 87 K and 20 K. After registering the files as closely as possible, the data file for the mirror in the dewar, in vacuum at room temperature (RTV), is subtracted from the data file for the mirror at 20 K. In the process, both systematic errors – window aberration and reference surface error – are eliminated. We report the cryo-change with piston, tilt, and focus (spherical) alignment errors subtracted.

The measured surface figures during the first cryo-cycle sometimes differ from those of the second and third. We conclude that initial mounting strains are modified by relative motions between parts of different CTE during the first cycle, but that a thermal stability is reached during this cycle. It is the data from the stabilized assembly in the second and third cycles that is used in this report.

Figure 6 shows the cryo-changes for BET2 mounted on the Cesium plate. The first cryo-change shown is the change from room temperature to 87 K; the second is the change from 87 K to 20 K. The third cryo-change shown is the total change from room temperature to 20 K.

Note that, for some values, a confidence limit is given. This is the repeatability (as one standard deviation) times a factor of three. See section 7C.

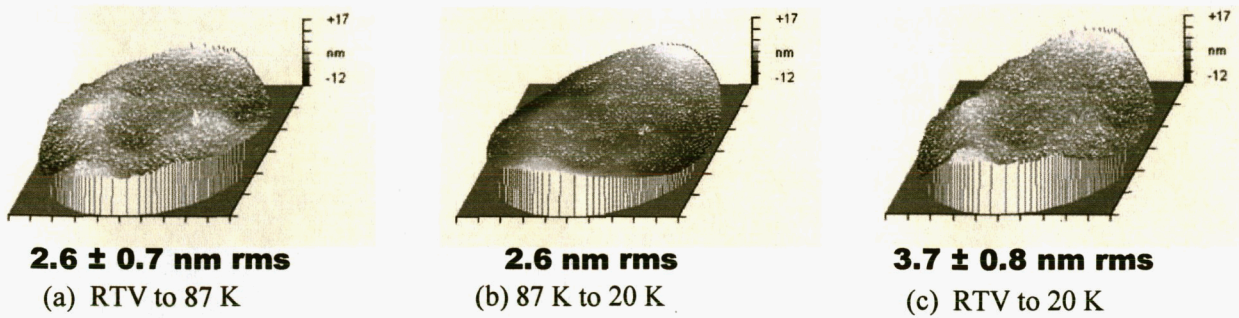


Figure 6: Cryo-changes of BET2, mounted to Cesic IF plate and kinematic Mount.

In an illustration of the repeatability of these measurements, figure 7 compares the mean 87K – RTV cryochange (from 6a above) to the four independent cryo-changes between RTV and 87K that went into it. Two salient points should be noted: 1) the similarity between the four cryo-changes (repeatability), and 2) the fact that the rms of the mean of the four (2.6 nm rms) is lower than the mean of the four rms statistics (2.9 nm rms).

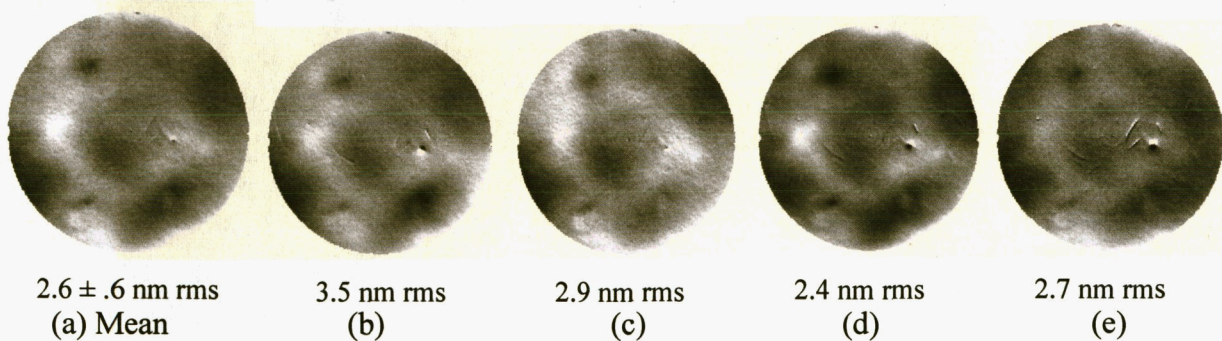


Figure 7: The mean and four individual cryo-changes, for BET2 on IF plate: 87K – RTV. a) the mean cryochange from RT to 87 K, b-e) the independent individual cryo-changes.

This reduction in the rms was seen every time in this program when measurements were averaged: when, for example, the twenty data sets that make up one individual stage measurement are averaged and the rms of this average file is compared to the mean of the twenty rms statistics. The explanation is suggested in a paper by Davies and Levenson¹⁰, in which an analogy is made between a wave front and a signal: in both cases a measurement is an approximation of the signal. The test result is the true measurand plus noise. In their paper,

Davies and Levenson develop an ingenious mathematical technique to isolate the noise of a wavefront measurement from its signal. In our case, the act of averaging reduces the noise. Since calculating the rms of a test result requires a squaring operation, the noise leads to an rms that is larger on average than the rms of the true surface. Averaging reduces the noise, as is well known. [MSOffice2]

When supported on the simple support, the cryochanges of the sintered silicon carbide mirror BET2, were similar to those mounted on the interface plate, as seen in figure 8:

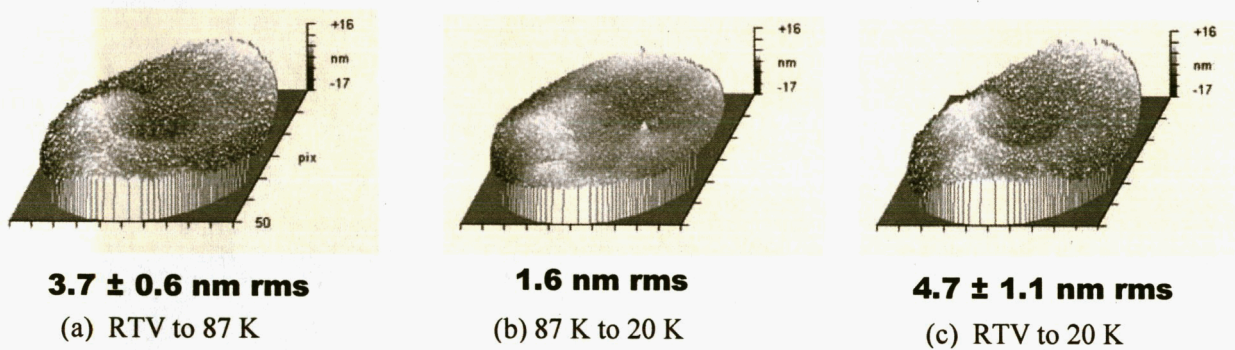


Figure 8: Cryo-changes of BET2, simply supported.

The cryochanges of the Cesium mirror, ECM3, mounted to the Cesium interface plate on the kinematic mount are given in figure 9. The mean cryo-change for the Cesium mirror, from room temperature to 20 K was larger (41.5 nm rms) than that of the sintered silicon carbide mirror.

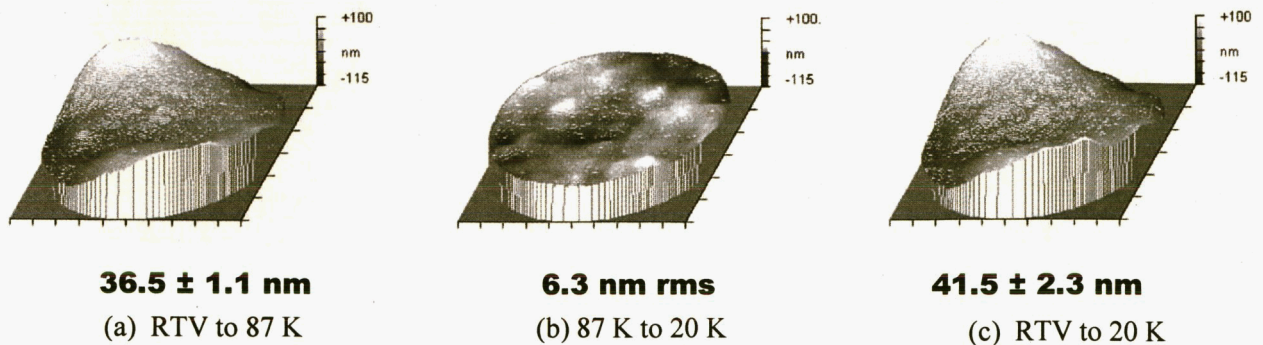


Figure 9: Cryo-changes of ECM3 on kinematic mount.

B Components of Uncertainty

The components of uncertainty fall into two broad types. First, we consider optical measurement uncertainties that relate to the correct measurement of the figure S of the mirror as it is in the dewar. Then we consider those thermo-mechanical components which affect the actual figure of the test mirror in unknown and uncontrolled ways. Table 1 lists these elements, and later sections support the dispositions listed in column three.

Table 1: Elements of Uncertainty

Category		Uncertainty element	Disposition
Optical	A	Short-term statistical (e.g., vibration)	Included in statistical uncertainty
	B	Long-term statistical (e.g., stratification of atmosphere)	Included in statistical uncertainty
	C	Data-set arithmetic (e.g., misregistration of data sets in equation 2)	Included in statistical uncertainty
	D	Cavity and transmission sphere misalignment	Included in statistical uncertainty
	E	Tilt of optic axis to window	Included in statistical uncertainty
	F	Uncertainty of correction file for reference surface in transmission sphere	Eliminated in equation 2
	G	Errors & uncertainty in PMI measurements and algorithms	Eliminated in equation 2
	H	Change in window aberration with cryostat temperature	Measured: less than 0.1 nm rms
Thermo-mechanical	I	Temperature gradients	Measured, then modeled in FEM: less than 0.4 nm rms
	J	Mounting strains	Eliminated in equation 2

Terms a-e are included in the statistical measure of uncertainty, calculated in the next subsection. Terms f-g are eliminated in the calculation of the cryo-change (equation 2). Term h was determined to be less than 0.1 nm rms in section 5, and is therefore ignored. Thus, the

systematic optical effects are all accounted for, either by being eliminated or by being measured. Therefore, a measure of the repeatability would capture all of the uncertainty in the measurement of the cryo-change that occurred. That statistical uncertainty is calculated in the next section.

C *Statistical uncertainty (repeatability) of cryo-changes*

In estimating the uncertainty of our optical measurements, we will include our knowledge of earlier measurements of a silicon mirror – Shafer’s SLMS mirror, also 600 mm radius, having used the exact same procedures⁴. When we include the SLMS series, and exclude those initial cycles where the surface figure differed from the later cycles (see section 7A, earlier), we have twenty independent cryo-changes (illustrated in figure 5) between RTV and 87K.

Table 2 lists, first, the independent cryo-changes between RTV and 87K, and, second, the independent changes between RTV and 20 K, together with the statistics of the measurements of those cryo-changes. The *mean* Δ is the calculated average rms cryo-change for the number, n , of independent cryo-changes making up the mean. (Once again, note that the mean of the rms values for the n trials is larger than the rms of their averaged data sets -- as given in figures 6, 8, and 9.)^[MSOffice3] The standard deviation (Std dev) is given in column four. Since the mean has a lower uncertainty than the individual measurements, the standard deviation of the individual measurements is divided by the square root of n to obtain the statistic known as the “standard error of the mean” (u_c mean), which is our estimate of the standard uncertainty of the reported rms. The expanded uncertainty (U_{3k}), with an expansion factor of three, is given in the final column and is quoted in figures 6, 8, and 9 as the confidence interval.

The standard uncertainty of our measure of the cryo-change from RT to 87 K for the sintered silicon carbide mirror, BET2, mounted to the interface plate and kinematic mount is, then, 0.23 nm rms; and the expanded uncertainty, with $k = 3$, is 0.7 nm rms.

Table 2: Statistical Uncertainty of Cryo-changes

87K-RTV	Mean Δ (<i>nm rms</i>)	n	Std dev	u_c mean	U_{3k} of the mean
SLMS	5.1	6	0.51	0.21	0.6
BET2k	2.9	4	0.46	0.23	0.7
BET2s	4.0	3	0.34	0.20	0.6
ECM3s	34.8	3	0.50	0.30	0.9
ECM3k	36.5	4	0.71	0.36	1.1
20K-RTV					
BET2k	4.0	2	0.37	0.26	0.8
BET2s	5.0	2	0.50	0.35	1.1
ECM3s	40.3	2	1.00	0.71	2.1
ECM3k	41.5	3	1.30	0.75	2.3

The fact that the measurement procedures are the same for the measurements of the RTV–20K cryo-changes gives us the confidence to calculate the uncertainties in the same way, even though the number of independent measurements of the RTV-20K cryo-change was low. The standard uncertainty for the cryo-change in BET2k between RT and 20 K is thus, 0.26 nm rms, with an expanded uncertainty of 0.8 nm rms.

***E* Thermo-mechanical components of Uncertainty**

Thermal gradients and mounting strains (including those of thermal straps) constitute a second type of uncertainty. The thermal gradients were measured by eight temperature-sensing diodes, including two diodes on the edge of the mirror, near the front surface. The temperatures were

placed into a FEA model, and the resulting strains calculated. With a gradient across the front surface of 0.1 K, as was found in our tests, the resultant SFE was less than 0.4 nm rms. When a 1 K gradient across the surface was modeled in the FEA model (with no CTE difference between substrate and cladding), the resultant SFE was about 4 nm rms. But since the true gradient was an order of magnitude less, we conclude that the standard uncertainty due to temperature gradients is below our level of concern.

A basic experiment illustrates the sensitivity of these mirrors to the details of their mounting. BET2 was placed repeatedly into the simple support mount by lifting and lowering it with a laboratory jack. After each well-centered replacement, the SFE was measured at RTP. The standard deviation of the rms value was 1.2 nm: *i.e.*, larger than the standard deviation between individual thermal cycles. Apparently, minute changes in the stresses imparted by the separate, almost identical mountings lead to an uncertainty that is of the same scale as the uncertainties in the measurements of Table 2. It is similar minute adjustments of strain and position that lead to the phenomenon, noted earlier, of stability in surface figure being reached only after the first cryocycle. After the first cycle, surface figure error due to mounting strains is eliminated in the calculation of the cryo-change.

However, in calculation of the *in situ* SFE, such uncertainty of strains imparted to the mirror by its mount must be included, and we estimate the upper limit of the standard uncertainty of this component as 1.2 nm rms.

8 Uncertainty of *In-Situ* Surface Figure Error at cryo-temperature

The *in-situ* surface figure S is simply the measurement made at temperature with corrections made for the systematic effects. Here is an analysis of the uncertainty of an estimate of the *in-situ* S .

A *Uncertainty of the Reference Surface Correction*

The reference surface of the transmission sphere was measured twice: once by the Zygo Corporation and once by our laboratory. Both measurements were “absolute”: *i.e.*, without secondary reference surfaces. Both were made using the “Two Sphere Test”^{8,9}. Great care was taken in both laboratories to control the ten degrees of freedom in order to get near-perfect alignment of all axes of rotation and symmetry. Both laboratories tested the reference surface of the transmission sphere with the transmission sphere in place in the same interferometer unit that was used in the cryo-measurements reported here.

Zygo’s laboratory used as their second sphere a convex reference mirror of low SFE, giving a shorter cavity than was used in our tests. GSFC used the SLMS mirror, with a higher SFE, but with the same length cavity as was used in the cryo-tests. Both laboratories found the deviation from perfect sphericity of the reference surface to be 4.3 nm rms. A rigorous calculation of the uncertainty has so far proved beyond the capabilities of both Zygo and GSFC. The product of both tests was a file representing the transmission sphere error. This file is to be subtracted from the raw averaged measurements. Our best estimate of the uncertainty of our correction is to subtract both files from several different measurements, to see what the difference is. This is really a sample size of only two independent measurements (one degree of freedom), but it is the best we can do.

Both the Zygo 2-sphere correction file and the GSFC 2-sphere correction file were subtracted from eight measurements at room temperature, from each of the four combinations of two GA test mirrors on two supports. The difference between the two corrections was found for each file. The eight differences thus found were averaged for our estimate of the standard uncertainty of the correction, with consistent results. The average and the standard uncertainty for correction of reference surface error is 0.5 nm rms.

B Window Aberration Correction

We can use the same method for determining the uncertainty of the window correction; and in this, we have more data to use. In the four series of measurements, there were nine pairs of measurements taken sequentially of the test optic at RTP (without window) and at RTV (window and vacuum). Subtracting these two measurements gives us the window effect, E_W :

$$E_W = M_{RTV} - M_{RTP} \quad (3)$$

Nine pairs of measurements yield nine estimates of E_W , which are averaged to find our best estimate of the correction factor.

A good measure of the uncertainty of this correction is obtained by subtracting from one common file the individual window effect files – nine times for the nine files. The standard deviation in the results obtained is a measure of the uncertainty. This calculation was repeated four times with four representative files, with consistent results. The average standard uncertainty for correction of the window aberration is 0.8 nm rms.

C Calculated in-Situ SFE

When the surface figure error map for any measurement at 20 K has the reference surface correction and the window aberration correction subtracted from it, the resultant SFE, the *in-situ* SFE, is estimated. During the very first excursion of BET2 to 20 K, delaminations developed in the CVD coating of SiC, delaminations due to a well-understood error in fabrication (correctable in future mirrors); and the ambient condition SFE had degraded to 15.8 nm rms. Corresponding to this ambient condition SFE, the SFE at 20 K was found to be tk nm rms.

D Combined standard uncertainty

The components of the combined standard uncertainty are listed and estimated in Table 3.

Table 3: Uncertainty Components for In-Situ Calculation of SFE

Uncertainty Component	Estimated u_i (nm rms)
Statistical	0.3
thermo-mechanical	1.2
Other interferometer absolute errors[MSOffice4]	< 0.5*
Reference sphere correction	0.5
Window corrections	0.8
Combined Standard Uncertainty	1.6 nm rms

* Upper bound given by the Zygo corporation

Therefore, the combined standard uncertainty for estimates made with our current data of the *in-situ* surface figure error of the test optics at 87 K and 20 K is 1.6 nm rms .[MSOffice5]

ACKNOWLEDGEMENTS

The authors gratefully acknowledge the assistance of the European Space Agency and the James Webb Space Telescope. Our thanks also to Galileo Avionica, ECM, and the Schafer Corporation; and to Chip Frohlich, Chris Chrzanowski, and Badri Shirgur of the Swales Corporation, Beltsville MD, and to Joe McMann of Mantech Systems Engineering Corp., Greenbelt, for their expert assistance on many aspects of this program. Thanks also to Barbara Carr and Chris Evans of Zygo Corp., Middlefield CT. And special thanks to Ulf Griesmann, NIST, for his valuable discussions on uncertainty.

Mention of trade names or commercial products does not constitute endorsement or recommendation by NASA.

REFERENCES

1. B. Taylor, C.E. Kuyatt, "Guidelines for Evaluation and Expressing the Uncertainty of NIST Measurement Results", NIST Technical Note 1297, 1994
2. ISO, *Guide to the Expression of Uncertainty in Measurement*, International Organization for Standardization, Geneva, Switzerland, 1993.
3. Marc T. Jacoby, *et. al.*, "Helium cryo-testing of a SLMSTTM (silicon lightweight mirrors) athermal optical assembly, *Proc SPIE 5180, Optical Manufacturing and Testing V*, ed. Phil Stahl, pp199-210, 2003
4. P. Blake, R. G. Mink, D. Content, P. Davila, F. D. Robinson, S. R. Antonille, "Techniques and uncertainty analysis for interferometric surface figure error measurement of spherical mirrors at 20K", *Proc SPIE, 5180, Optical Manufacturing and Testing V*, ed. Phil Stahl, pp188-198, 2003.
5. G. Mondello, A. Novi, C. Devilliers, "Development of sintered-SiC and C/SiC mirrors for cryogenic telescope", *SPIE Proc. 5494, Optical Fabrication, Metrology, and Material Advancements for Telescopes*, ed. E. Atad-Ettinger and P. Dierickx, pp 311-318
6. C. Chrzanowski, C. Frohlich, B. Shirgur, R. Mink, "Design and structural/optical analysis of a kinematic mount for the testing of silicon carbide mirrors at cryogenic temperatures", *Proc. SPIE Vol. 5528, Space Systems Engineering and Optical Alignment Mechanisms*; ed. Lee D. Peterson, Robert C. Guyer, p. 204-214, 2004

-
7. P. Blake, J. Chambers, R. G. Mink, D. Content, P. Davila, F. D. Robinson, C. Chrzanowski, B. Shirgur, C. Frohlich, "Cryogenic system for interferometry of high-precision optics at 20 K: Design and performance", to be presented Proc SPIE, *Cryogenic Optical Systems And Instruments XI*, ed. Jim Heaney, Lawrence Burriesci, August, 2005.
 8. J. E. Greivenkamp, J.H. Bruning, "Phase Shifting Interferometers", in *Optical Shop Testing*, 2nd ed., D. Malacara, ed., pp577-580, John Wiley & Sons, NY, 1992
 9. K. Elssner, R. Burow, J. Grzanna, R.Spolaczyk, "Absolute Sphericity Measurement," *Applied Optics*, **28**, pp 4649-4661, 1989
 10. A. Davies, M.S. Levenson, "Estimating the root mean square of a wave front and its uncertainty", *Applied Optics*, **40**, pp 6203-6209, 2001
-